Amino Acids (2012) 42:427–440
DOI 10.1007/s00726-011-1013-0

ORIGINAL ARTICLE

The activation of hepatic and muscle polyamine catabolism improves glucose homeostasis

Taina Koponen · Marc Cerrada-Gimenez · Eija Pirinen · Esa Hohtola · Jussi Paananen · Susanna Vuohelainen · Maija Tusa · Sini Pirnes-Karhu · Sami Heikkinen · Antti Virkamäki · Anne Uimari · Leena Alhonen · Markku Laakso

Received: 17 March 2011 / Accepted: 26 May 2011 / Published online: 4 August 2011

Abstract The mitochondrial biogenesis and energy expenditure regulator, PGC-1α, has been previously reported to be induced in the white adipose tissue (WAT) and liver of mice overexpressing spermidine/spermine N^1-acetyltransferase (SSAT). The activation of PGC-1α in these mouse lines leads to increased number of mitochondria, improved glucose homeostasis, reduced WAT mass and elevated basal metabolic rate. The constant activation of polyamine catabolism produces a futile cycle that greatly reduces the ATP pools and induces 5′-AMP-activated protein kinase (AMPK), which in turn activates PGC-1α in WAT. In this study, we have investigated the effects of activated polyamine catabolism on the glucose and energy metabolisms when targeted to specific tissues. For that we used a mouse line overexpressing SSAT under the endogenous SSAT promoter, an inducible SSAT overexpressing mouse model using the metallothionein I promoter (MT-SSAT), and a mouse model with WAT-specific SSAT overexpression (aP2-SSAT). The results demonstrated that WAT-specific SSAT overexpression was sufficient to increase the number of mitochondria, reduce WAT mass and protect the mice from high-fat diet-induced obesity. However, the improvement in the glucose homeostasis is achieved only when polyamine catabolism is enhanced at the same time in the liver and skeletal muscle. Our results suggest that the tissue-specific targeting of activated polyamine catabolism may reveal new possibilities for the development of drugs boosting mitochondrial metabolism and eventually for treatment of obesity and type 2 diabetes.

T. Koponen, M. Cerrada-Gimenez, L. Alhonen, M. Laakso contributed equally to this work

Electronic supplementary material The online version of this article (doi:10.1007/s00726-011-1013-0) contains supplementary material, which is available to authorized users.

T. Koponen (✉) · M. Cerrada-Gimenez · E. Pirinen · S. Vuohelainen · M. Tusa · S. Pirnes-Karhu · S. Heikkinen · A. Uimari · L. Alhonen
Biotechnology and Molecular Medicine, A. I. Virtanen Institute for Molecular Sciences, Biocenter Kuopio, University of Eastern Finland, Kuopio Campus, P.O. Box 1627, 70211 Kuopio, Finland
e-mail: taina.e.koponen@uef.fi

M. Cerrada-Gimenez · E. Pirinen · J. Paananen · M. Tusa · S. Heikkinen · M. Laakso
Department of Medicine, University of Eastern Finland, Kuopio Campus, 70211 Kuopio, Finland

E. Pirinen
Ecole Polytechnique Federale de Lausanne, Laboratory for Integrative and Systems Physiology, 1015 Lausanne, Switzerland

E. Hohtola
Department of Biology, University of Oulu, 90014 Oulu, Finland

S. Heikkinen
Department of Biosciences, University of Eastern Finland, Kuopio Campus, 70211 Kuopio, Finland

A. Virkamäki
Mehiläinen Diabetes Clinic, Pohj. Hesperinkatu 17C, Helsinki 00260, Finland

Keywords Polyamine catabolism · Transgenic mouse · White adipose tissue · Energy metabolism · AMPK · PGC-1α · Mitochondria

Abbreviations

AMPK	5′AMP-activated protein kinase
aP2	Fatty acid binding protein 4
BAT	Brown adipose tissue
GLUT4	Glucose transporter type 4
HFD	High-fat diet
MT	Metallothionein
mtDNA	Mitochondrial DNA
OXPHOS	Oxidative phosphorylation
PGC-1α	Peroxisome proliferator-activated receptor γ coactivator 1α
PPARγ	Peroxisome proliferator-activated receptor γ
Sirt1	Silent mating type information regulation 2 homolog
SSAT	Spermidine/spermine N^1-acetyltransferase
UCP	Uncoupling protein 1
WAT	White adipose tissue

Introduction

The natural polyamines (putrescine, spermidine and spermine) are cationic compounds found in all eukaryotic cells and in most prokaryotes. Polyamines are known to be crucial for the growth and proliferation of mammalian cells (Jänne et al. 2006). Polyamine metabolism is a closed cycle formed by the biosynthetic and catabolic branches. There are three rate-limiting enzymes in the polyamine metabolism; two of them, ornithine decarboxylase and *S*-adenosyl-L-methionine decarboxylase, belong to the biosynthetic pathway. The third rate-limiting enzyme is spermidine/spermine N^1-acetyltransferase (SSAT) that controls the catabolism of polyamines. The polyamine cycle consumes energy, a total of four ATP equivalents, two during the production of *S*-adenosy-L-methionine and two in the form of acetyl-CoA used as a cofactor of SSAT.

To study how polyamine catabolism activation affects the organism, we generated two different mouse lines with ubiquitous SSAT expression. The SSAT mouse line uses the endogenous SSAT promoter to regulate the transgenic construct (Pietilä et al. 1997), while the MT-SSAT mouse line uses a heavy metal-inducible promoter, the metallothionein I promoter (Suppola et al. 1999). These two mouse lines show remarkable phenotypic characteristics, such as loss of hair at an early age, reduced white perigonadal white adipose tissue and alterations in the different polyamine pools expected after SSAT overexpression, putrescine accumulation and decreased spermidine and spermine level (Pietilä et al. 1997; Suppola et al. 1999; Pirinen et al. 2007). A completely unexpected finding was that the activation of polyamine catabolism in the SSAT transgenic mice caused increased number of mitochondria in WAT, higher basal metabolic rate and increased insulin sensitivity (Pirinen et al. 2007). These changes are believed to be attributable to the increased 5′AMP-activated protein kinase (AMPK) and PGC-1α expression in the WAT. AMPK is the major sensor of the cellular energy state and functions by stimulating the ATP producing pathways and inhibiting pathways and cellular functions consuming ATP (Winder and Hardie 1999). AMPK is an activator of the peroxisome proliferator-activated receptor γ coactivator 1α (PGC-1α) (Attie and Kendziorski 2003), which is the master regulator of mitochondrial biogenesis and energy expenditure (Cantó and Auwerx 2009). The activation of hepatic polyamine catabolism has also been noted to cause an increase of PGC-1α, which in the liver stimulates the expression of CYP7A1, the rate-limiting gene of the bile acid synthesis and, therefore, enhances cholesterol elimination (Pirinen et al. 2010), In addition, overexpression of PGC-1a in the liver of the MT-SSAT transgenic mice has been associated with improved glucose homeostasis (Cerrada-Gimenez et al. 2010).

Disturbances of cellular metabolism are often linked to mitochondrial dysfunction, which are the primary cellular site for energy production. It has been postulated that mitochondrial abnormalities predispose to the development of common metabolic disorders such as type 2 diabetes and obesity (Auwerx 2006). In line with this hypothesis, diabetic patients and their offspring present reduced number of mitochondria (Song et al. 2001; Morino et al. 2005), lowered oxidative capacity (Petersen et al. 2004, 2005) and expression of OXPHOS genes in skeletal muscle (Patti et al. 2003; Mootha et al. 2003). Reduced mitochondrial capacity may be mediated by PGC-1α, which is indeed downregulated in the skeletal muscle of diabetic patients (Patti et al. 2003) and in the WAT of insulin-resistant and morbidly obese people (Hammarstedt et al. 2003; Semple et al. 2004). Currently, methods that aim to increase energy metabolism via increasing the number and function of mitochondria are under an intensive investigation as possible therapeutics for type 2 diabetes and obesity research (Goldman et al. 2010; Vial et al. 2010).

In the current study, we investigated how the activation of polyamine catabolism targeted to different tissues affects glucose and energy metabolisms by comparing two transgenic mouse lines having ubiquitous SSAT overexpression (SSAT and MT-SSAT) (Pietilä et al. 1997; Suppola et al. 1999) to mice having WAT targeted SSAT overexpression (aP2-SSAT). Our study shows that enhanced polyamine catabolism in the liver and skeletal muscle improves glucose and cholesterol homeostasis,

whereas adipose tissue-specific SSAT overexpression leads to protection from high-fat diet-induced obesity, thereby improving whole-body energy metabolism.

Materials and methods

Generation of transgenic mice

The generation of transgenic UKU165b mice (SSAT mice) overexpressing SSAT under an endogenous SSAT promoter and UKU181 mice (MT-SSAT mice) overexpressing SSAT under a mouse metallothionein I promoter have been described previously (Pietilä et al. 1997; Suppola et al. 1999). The transgenic mouse line UKU395 (aP2-SSAT) was generated by transferring the aP2-SSAT transgene construct into oocytes of DBA/2 × BALB/c females mated with CDF1 males by using the standard microinjection technique (Hogan et al. 1986). The fat-specific SSAT expression transgene construct was produced by combining the promoter of fatty acid binding protein 4 (aP2) gene and the genomic clone of SSAT. The 5.5-kb fragment of aP2 promoter covering the region from −5499 to +46 was PCR amplified from DBA_2 mouse genomic DNA with the primers 5′-CTAGTCGAGGAATCGCACAGAGCCATG-3′ and 5′-CTACTCGAGAGCTGTCTTCCAGGTGAG-3′. The 3.1-kb clone for SSAT, containing all the exons and introns of the gene and 196 bp of 5′UTR and 210 bp of 3′UTR, was PCR amplified from 129 SVJ mouse genomic DNA with the primers 5′-TACGTCGACGTCTT GCCACTTCTTAGC-3′ and 5′-CTAGCGGCCGCACC ACCTTGTTCTTCATC-3′. SSAT gene and the aP2 promoter were inserted into the vector CMV/Myc/Cyto (Invitrogen, San Diego, CA) using *Sal*I and *Not*I sites. For microinjection, the 8.6-kb *Sal*I–*Not*I aP2-SSAT insert was used.

Mice were housed on 12 h light/dark cycle at 22 ± 1°C and were fed a regular laboratory chow (Lactamin, Sweden) or a high-fat diet (HFD) providing 42% of calories from fat (Altromin, Germany). All the animals used in this study were females (unless otherwise stated) and aged from 4 to 8 months. The study protocols were approved by the Animal Care and Use Committee at the Provincial Government of Eastern Finland.

Histology

Mice were killed by cervical dislocation or CO_2 inhalation. Perigonadal WAT was removed from mice and fixed in 10% formaldehyde. Fixed samples were dehydrated and embedded in paraffin. Tissues were cut in 10 μm sections, mounted on slides and stained with hematoxylin and eosin or with oil red O.

Analysis of body composition and basal metabolic rate

Fat percentages were determined by magnetic resonance imaging (MRI) and using an Aedes program made with Matlab software (MathWorks, MA, USA). Basal metabolic rate was measured from 10 to12 h fasted mice by indirect calorimetry as described previously (Pirinen et al. 2007).

Polyamine levels and SSAT activity

Polyamines were determined by using high-performance liquid chromatography (HPLC) (Hyvönen et al. 1992). SSAT activity was assayed by the incorporation of [^{14}C]-acetyl-CoA into spermidine (Libby et al. 1991). SSAT activity and polyamine concentrations were normalized to DNA amount assayed by modified Burton's method (Giles and Myers 1964).

Tolerance tests and analytical methods

Laboratory parameters for glucose and pyruvate tolerance tests were determined after 10–12 h of fasting. In all tolerance tests, nonanesthetized mice were subjected to intraperitoneal injections of 2 mg/g glucose or pyruvate and plasma samples were taken from the tail vein at specified time points.

Fasting plasma or serum samples were taken from the saphenous vein of 12 h fasted nonanesthetized mice. Blood levels of serum-free fatty acids were measured by using a colorimetric detection kit (Wako Diagnostics, VA, USA), and plasma triglycerides and cholesterol levels were colorimetrically measured using Microlab 200 analyzer (Merck, Germany). Plasma glucose was determined microfluorometrically (Passonneau and Lowry 1993) and plasma insulin levels by using a rat insulin enzyme-linked immunosorbent assay (ELISA) kit (Chrystal Chem Inc, IL, USA) with mouse insulin as a standard.

Illumina analysis

Total RNA from perigonadal WAT of fed mice was isolated using an RNeasy mini kit (QIAGEN, Germany), and RNA quality was checked with Agilent Analyzer (Agilent RNA 6000 Nano). Hybridization was performed at the Finnish Microarray and Sequencing Center (Turku, Finland) according to Illumina Whole-Genome Gene Expressio Direct Hybridization Assay Guide. Illumina Mouse WG-6 version 2 microarrays were used.

Data analyses were performed using R statistical software version 2.12.1 (R Dev Core Team 2009), Bioconductor version 2.41 (Gentleman et al. 2004) and Lumi analysis package version 2.2.1 (Du et al. 2008). Importing and quality assessment of the data was performed using

Lumi package. Variance stabilizing transformation (VST) (Lin et al. 2008) and robust spline normalization (RSN) were used to preprocess and normalize the data. Non-specific filtering was used to filter out less informative probes including probes not linked to genes and probes with small variance across samples. Of the original 45,281 probes 10,856 were retained after filtering, representing the same number of unique genes. Linear Models for Microarray Data (limma) version 3.6.9 analysis package (Smyth 2004) was used to detect the differentially expressed genes between groups, using fitting of linear models and applying empirical Bayes smoothing to each probe. Benjamini–Hochberg false discovery rate (FDR) was used to adjust results for multiple comparisons (Benjamini and Hochberg 1995). FDR-adjusted p value ≤ 0.05 was considered to be statistically significant.

Gene set enrichment analysis of significantly differentially expressed genes was performed to identify over-represented gene ontology (GO) terms and KEGG pathways. Hyper geometric test from Bioconductor Category package version 2.16 was used for enrichment analysis.

Illumina gene expression microarray data are available at ArrayExpress under the accession number E-MTAB-569.

Quantitative PCR and mtDNA analysis

Total RNA from perigonadal WAT of fed mice was isolated using an RNeasy mini kit (QIAGEN) and liver with Tri Reagent (Molecular Research Center Inc., OH, USA) according to the manufacturer's protocol. Total RNA was treated with DNA-free (Applied Biosystems, CA, USA). The absence of genomic DNA was verified by a lack of PCR amplification with primers recognizing numerous GAPDH (glyceraldehyde-3-phosphate dehydrogenase) pseudogens. Total RNA was transcribed to cDNA by the use of a high-capacity cDNA archive kit (Applied Biosystems). Quantitative real-time (RT) PCRs were performed using 12 ng (RNA equivalents) of cDNA as a template, gene-specific primers and probes, and TaqMan reagents with StepOnePlus instrument (Applied Biosystems). Running conditions were 2 min at 50°C, 10 min at 95°C and 40 cycles of 15 s at 95°C and 1 min at 60°C. All primers and probes were designed using an assay-by-design system (Applied Biosystems).

Mitochondrial DNA (mtDNA) analysis was isolated from WAT using proteinase K and phenol–chloroform–isoamyl alcohol extraction (Chomczynski and Sacchi 1987). The isolated mtDNA was quantified by measuring the ratio of the mitochondrial gene (16S RNA) to a nuclear gene (hexokinase II intron 9) using quantitative RT-PCR as described previously (Pirinen et al. 2007).

Western blot analysis

Perigonadal WAT and liver tissue samples from fed mice were homogenized in RIPA-buffer containing 50 mM Tris–HCL of pH 7.6, 0.15 M NaCl, 1% Triton X-100, 1 mM phenylmethylsulfonyl fluoride in dimethyl sulfoxide, 10 mM Na_3VO_4, 100 mM NaF, 10 mM $Na_4P_2O_7$ and protease inhibitor cocktail (Roche Applied Science, Switzerland). As much as 20–50 μg of protein from WAT and liver were boiled for 5 min, subjected to sodium dodecyl sulfate-polyacrylamide gel electrophoresis (SDS-PAGE) and transferred onto polyvinylidene difluoride (PVDF) membranes. Membranes were blocked overnight with 5% non-fat milk in phosphate-buffered saline (PBS) containing 0.1% Tween. Blots were probed with PGC-1α (1:10000, Cell Signaling, MA, USA), phosphorylated α subunit of AMPK (1:1000, Cell Signaling) or actin (1:10000, Sigma). This was followed with appropriate HRP-conjugated secondary antibody and detection was done with an Amersham ECL Plus Western blotting detection kit (GE Healthcare, NJ, USA).

Data and statistical analyses

Statistical analyses were performed using Student's t test (two-tailed) except that one-way or two-way analysis of variance was used for comparisons of multiple groups (GraphPad Prism software, CA, USA). A p value of <0.05 was considered statistically significant. All data are expressed as mean ± standard errors of the means (SEM).

Results

SSAT activity and polyamine pools

SSAT transgenic mice had the highest level of SSAT activation in the WAT. Nonetheless, the liver and skeletal muscle also had elevated SSAT activity compared to wild-type mice (Pirinen et al. 2007) (see Fig. 1a). In the MT-SSAT transgenic mouse line, although SSAT expression was ubiquitous, the main affected organ was the liver, while skeletal muscle and WAT were less affected (see Fig. 1b). As expected, SSAT activation was only detected in WAT (see Fig. 1c) and BAT (data not shown) of aP2-SSAT transgenic mice. Changes in the polyamine pools, i.e., decreased spermine, and accumulation of putrescine and N^1-acetyl spermidine, were seen in the tissues affected by SSAT activation (see Table 1). However, although the level of putrescine was greatly increased, the spermidine and spermine pools remained unchanged in the WAT of aP2-SSAT.

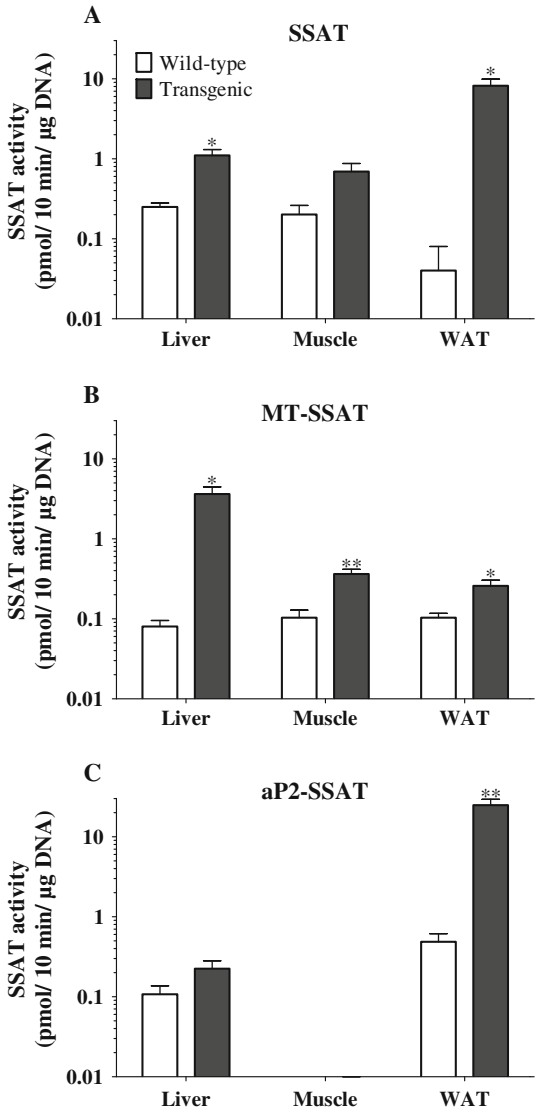

Fig. 1 SSAT activities in the liver, muscle and WAT from three different transgenic mouse lines with activated polyamine catabolism. Results are expressed as mean ± SEM from **a** SSAT and **b** MT-SSAT (3 mice per genotype), and **c** aP2-SSAT (3–16 mice). $*p < 0.05$, $**p < 0.005$, $***p < 0.0001$. Note that the *y*-axis is depicted in log10 scale. SSAT data are reprinted with kind permission from the original publishers (Pirinen et al. 2007)

Growth and body composition of the mice

One of the most striking phenotypic characteristics of ubiquitously activating the polyamine catabolism is that transgenic mice, both SSAT and MT-SSAT, had a 50% reduced lifespan (Cerrada-Gimenez et al. 2010) (see Fig. 2a, b). However, in aP2-SSAT mice, with the activation of polyamine catabolism targeted to the WAT, had no alteration in the lifespan when compared with wild-type mice (see Fig. 2c).

In all three transgenic mouse lines, there was a clear decrease in the perigonadal WAT (Pirinen et al. 2007) (see Fig. 2d). Corresponding with reduced fat mass, MT-SSAT transgenic mice appeared to be slightly lighter than controls. Although, body weight of SSAT mice was slightly lower compared to that of their littermates up to 8 weeks, by the age of 3–4 months, female SSAT mice had the tendency to be heavier (Pirinen et al. 2007). Female aP2-SSAT mice had a tendency to be heavier after the age of 4 months (data not shown). A more detailed histological examination of the perigonadal WAT demonstrated major macroscopic alterations in the three transgenic mouse lines. The fat depots in WAT of transgenic mice resembled the smaller multilocular depots usually found in the BAT (Pirinen et al. 2007) (see Fig. 2e). Moreover, the mitochondrial amount in the WAT of SSAT and aP2-SSAT mice appeared to be increased (SSAT: 192 ± 28% wild-type [$p < 0.05$] (Pirinen et al. 2007); aP2-SSAT: 125 ± 5% wild-type [$p < 0.05$]). No other macrohistological alterations were observed in any other organs, including the BAT.

Energy expenditure

SSAT (Pirinen et al. 2007) and MT-SSAT transgenic mice had increased oxygen consumption compared to the wild-type littermates (see Fig. 2f). However, no changes in the basal metabolic rate were observed in the aP2-SSAT mice (see Fig. 2f).

Biochemical measurements of fasting mice

In the whole-body SSAT overexpression models, SSAT (Pirinen et al. 2007) and MT-SSAT, decreased fasting glucose and insulin plasma levels were seen (see Table 2). Moreover, the levels of fasting cholesterol and triglycerides were decreased (Pirinen et al. 2007, 2010). However, the aP2-SSAT mice did not show any alterations in the different blood metabolites when compared with the wild-type mice (see Table 2).

Glucose and pyruvate tolerance tests

Plasma glucose and insulin levels in SSAT (Pirinen et al. 2007) and MT-SSAT mice during glucose tolerance tests were significantly lower in all time points, demonstrating enhanced glucose tolerance compared to wild-type mice (see Fig. 3a, b, d). However, no change in glucose tolerance was observed in aP2-SSAT mice (see Fig. 3c, d).

As fasting glucose levels were reduced in SSAT and MT-SSAT mice, we investigated whether these mice have reduced gluconeogenesis. The SSAT mice had decreased hepatic expression of genes involved in the regulation of gluconeogenesis, such as phosphoenolpyruvate carboxykinase (Pepck) and glucose-6-phosphatase (G6PC1), whereas

Table 1 Polyamine levels in liver and WAT of the three mouse lines with activated polyamine catabolism

	Putrescine (pmol/μg DNA)	N^1-Ac Spermidine	Spermidine	Spermine
Liver				
SSAT				
Wild type	0.4 ± 0.1	ND	41.2 ± 3.2	30.4 ± 1.4
Transgenic	19.8 ± 1.8*	0.1 ± 0.01	46.9 ± 3.9	16.8 ± 0.5***
MT-SSAT				
Wild type	1.3 ± 0.3	ND	42 ± 1.7	35.7 ± 1.9
Transgenic	90.5 ± 12.2**	20 ± 7.5***	25.4 ± 4.7*	3.1 ± 0.3***
aP2-SSAT				
Wild type	ND	ND	22.4 ± NA	15.1 ± NA
Transgenic	ND	ND	21.7 ± 1	18.1 ± 0.6
WAT				
SSAT				
Wild type	7.9 ± 1.6	ND	95.6 ± 13.5	42.7 ± 4.9
Transgenic	175.8 ± 25.9*	1,107.4 ± 316.5	101.1 ± 5.6	22.9 ± 0.9*
MT-SSAT				
Wild type	1.5 ± 0.3	ND	21.9 ± 5.5	9.1 ± 2.8
Transgenic	31.3 ± 8.6*	ND	40.6 ± 12.95	12.5 ± 5.8
aP2-SSAT				
Wild type	26.9 ± 17.6	ND	69.3 ± 4.3	38.1 ± 4.9
Transgenic	262.9 ± 34.8*	5.2 ± 1.5	69.8 ± 10.4	24.3 ± 1.3

ND not detected, *NA* not available. Polyamine levels in WAT of SSAT mice are reprinted with kind permission from the original publishers (Pirinen et al. 2007)

$N = 3$, * $p < 0.05$, ** $p < 0.005$, *** $p < 0.0001$

MT-SSAT mice had elevated expression of these same genes (Cerrada-Gimenez et al. 2010) (see Fig. 5b). We further tested the in vivo rate of gluconeogenesis by performing a pyruvate tolerance test. The MT-SSAT mice revealed significantly lower plasma glucose levels in transgenic mice at all time points when compared with wild-type mice (see Fig. 3e).

High-fat diet

To test whether whole-body or adipose tissue-specific activation of polyamine catabolism protects from HFD-induced weight gain, we challenged SSAT and aP2-SSAT mice for 3 months with an HFD. Although the SSAT transgenic mice had increased food consumption, when fed either a normal chow or a high-fat diet (see Fig. 4a), under a high-fat diet the increase in body weight was only minor compared to wild-type mice (see Fig. 4b). The aP2-SSAT mice also gained less weight as compared to wild-type mice despite the fact that both phenotypes consumed similar quantities of food (see Fig. 4b). Nonetheless, as compared to the SSAT mice, aP2-SSAT mice gained slightly more weight.

Surprisingly, glucose tolerance was even further improved after HFD in SSAT mice (see Fig. 4c, d, g and h). In contrast, glucose tolerance was equally impaired after HFD in the aP2-SSAT and wild-type mice (see Fig. 4e, f, g and h).

Gene expression analyses

The Illumina microarray analyses were performed on WAT for all three transgenic and wild-type mice to investigate metabolic processes affected by the differential enhanced polyamine catabolism. Statistically differentially expressed (DE) genes between the groups were detected and further studied. When SSAT mice were compared with MT-SSAT mice, the top-ranked biological processes with the highest number of changes were in cellular lipid metabolic processes (26 DE genes), purine metabolic processes (20 DE genes) and glucose metabolic processes (19 DE genes) (see Supplementary Table 1). The biological processes with the highest number of changes when comparing the SSAT and the aP2-SSAT mice were nucleoside phosphate metabolic processes (10 DE genes), carbohydrate metabolic processes (8 DE genes) and brown fat cell differentiation (three DE genes) (see Supplementary Table 2). When the aP2-SSAT and the MT-SSAT mice were compared, the biological processes presenting most changes were cellular ketone metabolic processes (42 DE genes), lipid metabolic processes (16 DE genes) and glucose metabolic processes (15 DE genes) were the most enriched terms (see Supplementary Table 3).

We used quantitative RT-PCR to determine the expression of genes governing mitochondrial metabolic pathways, nuclear receptors and regulators of glucose uptake and oxidation in WAT and liver (see Fig. 5a, b,

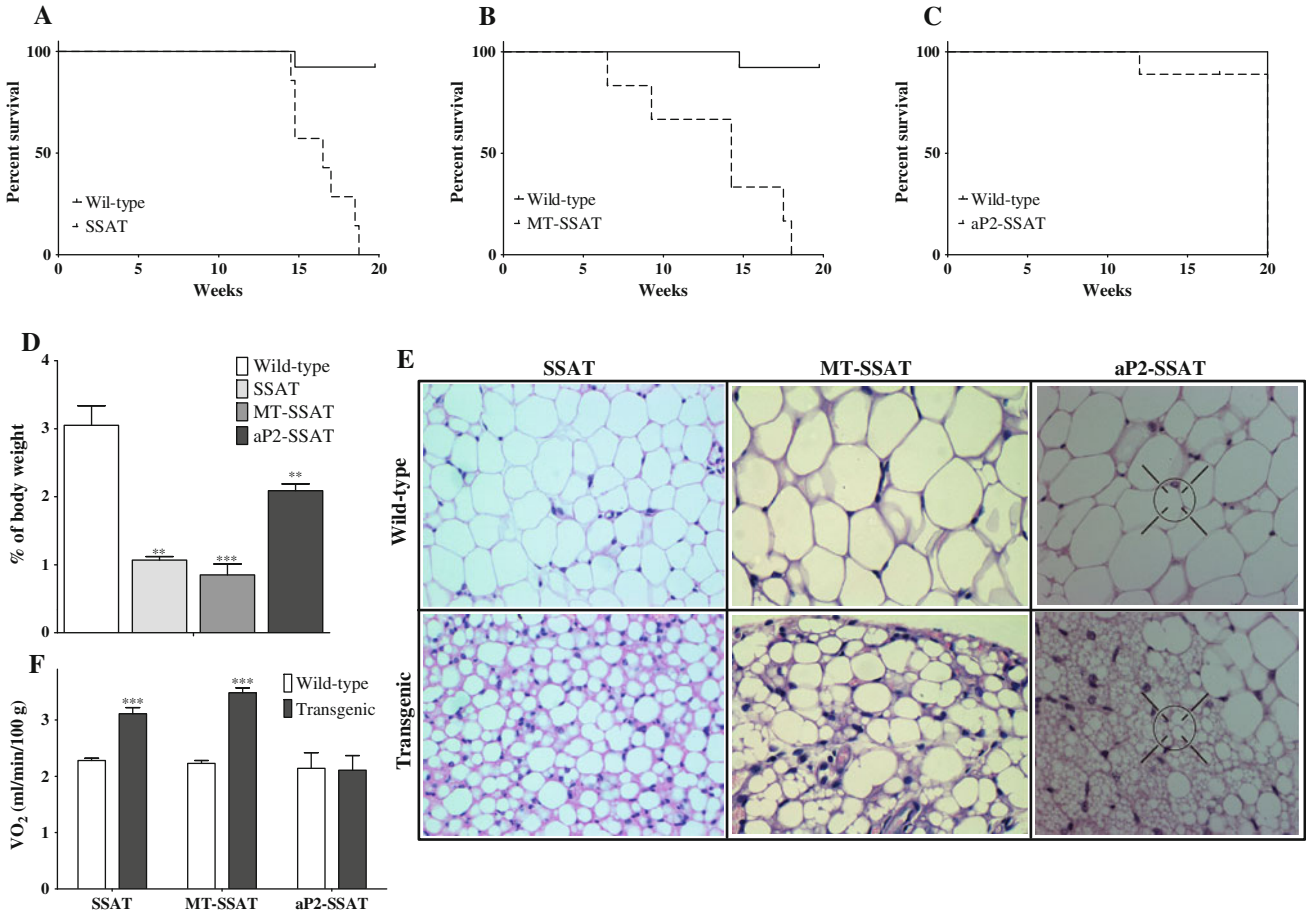

Fig. 2 Survival and body composition characteristics from three different transgenic mouse lines with activated polyamine catabolism. Survival curves of the **a** SSAT, **b** MT-SSAT and **c** aP2-SSAT transgenic mice. **d** Perigonadal WAT amounts from the SSAT, MT-SSAT and aP2-SSAT mice. **e** Histology of perigonadal WAT in MT-SSAT and aP2-SSAT mice. Images from the SSAT mice were taken at × 20 magnification, while those from the MT-SSAT and aP2-SSAT were taken using a × 40 magnification. **f** Energy expenditure (basal metabolic rate) of SSAT, MT-SSAT and aP2-SSAT mice. The oxygen consumption was measured by indirect calorimetry and the results are expressed per body weight. All the results are expressed as mean ± SEM from wild type ($N = 12$–103), SSAT ($N = 8$–13), MT-SSAT ($N = 4$–8) and aP2-SSAT ($N = 12$–83). $^{*}p < 0.05$, $^{**}p < 0.005$, $^{***}p < 0.0001$. MT-SSAT mice survival curve, and SSAT mice WAT histological images and basal metabolic rate values are reprinted with kind permission from the original publishers (Cerrada-Gimenez et al. 2011; Pirinen et al. 2007)

Table 2 Fasting blood metabolites from three different mouse lines with activated polyamine catabolism

	Glucose (mM)	Insulin (ng/μl)	Cholesterol (mM)	Triglycerides (mM)	Free fatty acids (mM)
SSAT					
Wild type	10.3 ± 0.4	0.6 ± 0.2	2.2 ± 0.2	1.4 ± 0.1	0.7 ± 0.05
Transgenic	8.5 ± 0.2***	0.3 ± 0.1*	1.4 ± 0.1*	1 ± 0.1*	0.7 ± 0.06
MT-SSAT					
Wild type	8.5 ± 0.4	0.42 ± 0.07	2.58 ± 0.08	1.39 ± 0.04	NA
Transgenic	6.9 ± 0.4*	0.26 ± 0.04	1.27 ± 0.02***	1.12 ± 0.04***	NA
aP2-SSAT					
Wild type	7.8 ± 0.4	0.4 ± 0.1	2.7 ± 0.2	1.3 ± 0.1	0.9 ± 0.2
Transgenic	8.3 ± 0.2	0.4 ± 0.2	2.8 ± 0.1	1.5 ± 0.07	0.9 ± 0.1

NA not available. SSAT data are reprinted with kind permission from the original publishers (Pirinen et al. 2007, 2010)

N(SSAT) = 12, N(MT-SSAT) = 6, N(aP2-SSAT) = 6–54. * $p < 0.05$, *** $p < 0.0001$

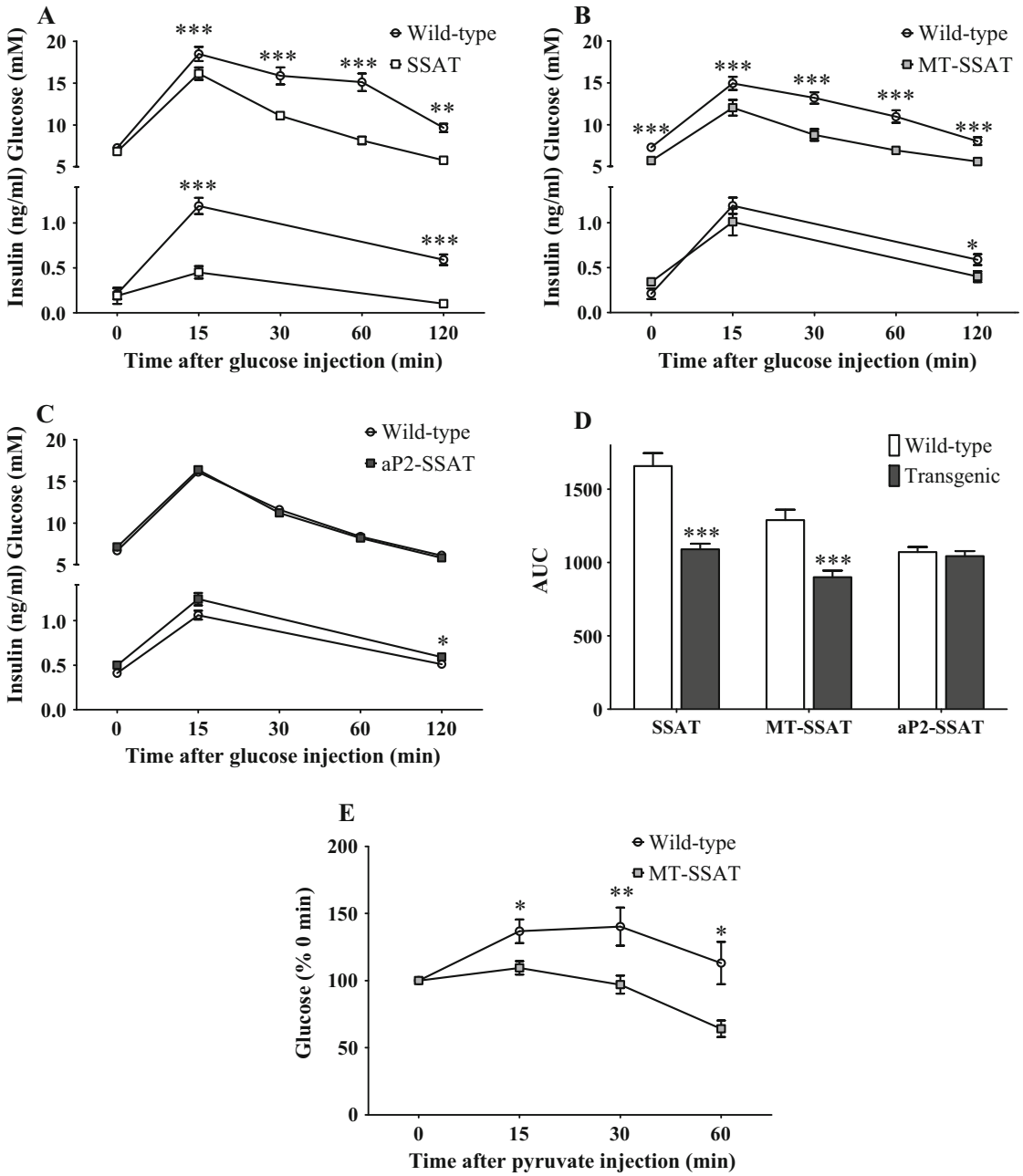

Fig. 3 Glucose tolerance test from three transgenic mouse lines with activated polyamine catabolism and pyruvate tolerance test from MT-SSAT transgenic mice. Glucose and insulin concentrations during the glucose tolerance test in **a** SSAT ($N = 12$), **b** MT-SSAT ($N = 12$) and **c** aP2-SSAT ($N = 54$–59). **d** AUC from the glucose levels during the glucose tolerance tests. The glucose tolerance tests were performed by injecting 12 h fasted mice intraperitoneally with 2 mg of D-glucose/g of body weight. **e** Pyruvate tolerance test of wild-type and MT-SSAT ($N = 12$) mice. The pyruvate tolerance tests were performed by injecting 10 h fasted mice intraperitoneally with 2 mg of sodium pyruvate/g of body weight. Data are expressed as mean ± SEM. *$p < 0.05$, **$p < 0.005$, ***$p < 0.0001$. SSAT mice glucose tolerance data are reprinted with kind permission of the original publishers (Pirinen et al. 2007)

respectively). The expression of PGC-1α was significantly elevated in the WAT of the three mouse lines and in the liver of the MT-SSAT mice (Pirinen et al. 2007, 2010). In the WAT of all three mouse lines, the nuclear factor stimulating fatty acid oxidation, PPARα, tended to be upregulated, as well as genes from the OXPHOS pathway, Ndufa1, Sdhb and Coxa4 (Pirinen et al. 2007) (see Fig. 5a). A known marker for adipocyte differentiation, PPARγ, was found significantly upregulated in the WAT of SSAT and MT-SSAT mice. In the liver from MT-SSAT, either in fed or fasted state, uncoupling protein 2 (UCP2), cytochrome P450, family 7, subfamily A, polypeptide 1 (Cyp7A1) and

PGC-1α were upregulated. In the SSAT mice, UCP2 was upregulated during fed state, while Cyp7A1 was upregulated in both states (Pirinen et al. 2010) (see Fig. 5b). No changes were observed in glucose metabolism or fatty acid metabolism in the BAT, liver or skeletal muscle of aP2-SSAT mice (data not shown).

Protein expression

Western blot analysis revealed that phosphorylated AMPK was elevated in the WAT of SSAT (Pirinen et al. 2007) and aP2-SSAT mice, while PGC-1α protein levels were increased in the WAT of all three transgenic mouse lines (Pirinen et al. 2007) and the livers from SSAT and MT-SSAT mice (Pirinen et al. 2010; Cerrada-Gimenez et al. 2010) (see Fig. 6).

Discussion

In the current study, we compared three transgenic mouse lines with activated polyamine catabolism targeted to different tissues: the SSAT mice with ubiquituous SSAT expression; the MT-SSAT mice with pancreas/liver targeted SSAT expression; and the aP2-SSAT mice with WAT-specific SSAT expression. The main findings were that enhanced polyamine catabolism in liver and skeletal muscle led to the suppression of gluconeogenesis and increased insulin sensitivity and enhanced glucose tolerance, and that the adipose tissue-specific activation of polyamine catabolism was sufficient to lead to reduction of WAT mass and protect the mice from HFD-induced weight gain.

Although the highest SSAT activation in the WAT was found in the aP2-SSAT mice, the changes in the adipose tissue metabolism from this particular mouse line were not as profound as those from the other two mouse models with whole-body polyamine catabolism activation. This observation suggests that the activation of polyamine metabolism in the liver and skeletal muscle may also affect the glucose and energy metabolisms in the WAT. Nonetheless, the WAT mass was reduced in all three studied mouse lines. Histological examination revealed that adipocytes from all three transgenic lines were smaller than wild type and widely populated with mitochondria. The expression of the key regulatory factor in adipogenesis, PPARγ, was upregulated in the WAT from all three transgenic mouse lines, indicating that the reduced adipocyte cell size was related to decreased accumulation of triglycerides, and not to impaired adipocyte differentiation. Therefore, as the mitochondrial number and the expression of genes involved in the OXPHOS and/or fatty acid oxidation increased, the adipocytes of the three transgenic mouse models were transformed from fat-storing white adipocytes into fat-burning brown adipocytes. In line with our results, Porter and colleagues presented that malonyl-CoA was reduced in the WAT of SSAT mice (Jell et al. 2007), and this would activate the rate-limiting enzyme in the fatty acid oxidation, carnitine palmitoyltransferase I (McGarry and Brown 1997).

The energy expenditure, measured as oxygen consumption, was enhanced in the mouse lines with whole-body activation of polyamine catabolism, whereas no changes were seen in the aP2-mice. It should be noted that, metabolically, WAT is quite an inactive organ, making it difficult to measure alterations in the oxygen consumption produced by WAT. As increased oxygen consumption is normally caused by elevated number of mitochondria in combination with increased oxidative capacity and/or fatty acid oxidation, these factors most likely contribute to enhance energy expenditure in these mouse models. Therefore, the present data may suggest that ubiquitous activation of polyamine catabolism may be a promising target pathway to increase energy expenditure.

Female SSAT and MT-SSAT mice presented increased insulin sensitivity and glucose tolerance. Significantly reduced fasting insulin levels have also been reported in male MT-SSAT mice (Cerrada-Gimenez et al. 2010). In contrast, the aP2-SSAT mice did not present improved glucose homeostasis. The Illumina gene expression microarray analyses revealed that the highest number of changes between the SSAT or MT-SSAT compared to the aP2-SSAT mice appeared in the glucose/carbohydrate metabolic processes. Moreover, consistent with increased insulin action in female SSAT and MT-SSAT mice, gluconeogenesis was suppressed in the livers of SSAT and MT-SSAT mice, since they had significantly reduced fasting glucose levels (Pirinen et al. 2007) and lower hepatic glucose production during a pyruvate tolerance test. However, the expression profile of some hepatic genes involved in gluconeogenesis had contradictory patterns in the SSAT (downregulated) and the MT-SSAT (upregulated) mice. Nonetheless, this phenomenon could be, most likely, a compensatory mechanism due to the low glucose levels observed in transgenic mice. In line with increased hepatic insulin sensitivity, plasma triglyceride contents were significantly reduced in female SSAT (Pirinen et al. 2010) and MT-SSAT mice, most likely as a response to insulin that is known to enhance hydrolysis of triglycerides from either hepatic very low-density lipoproteins or dietary chylomicrons. However, the specific mechanisms resulting in decreased gluconeogenesis and increased insulin action need to be investigated in more detail.

Pirinen et al. (2010) have suggested that the mechanism leading to low cholesterol levels in SSAT mice could be the induction of rate-limiting enzyme of bile acid synthesis,

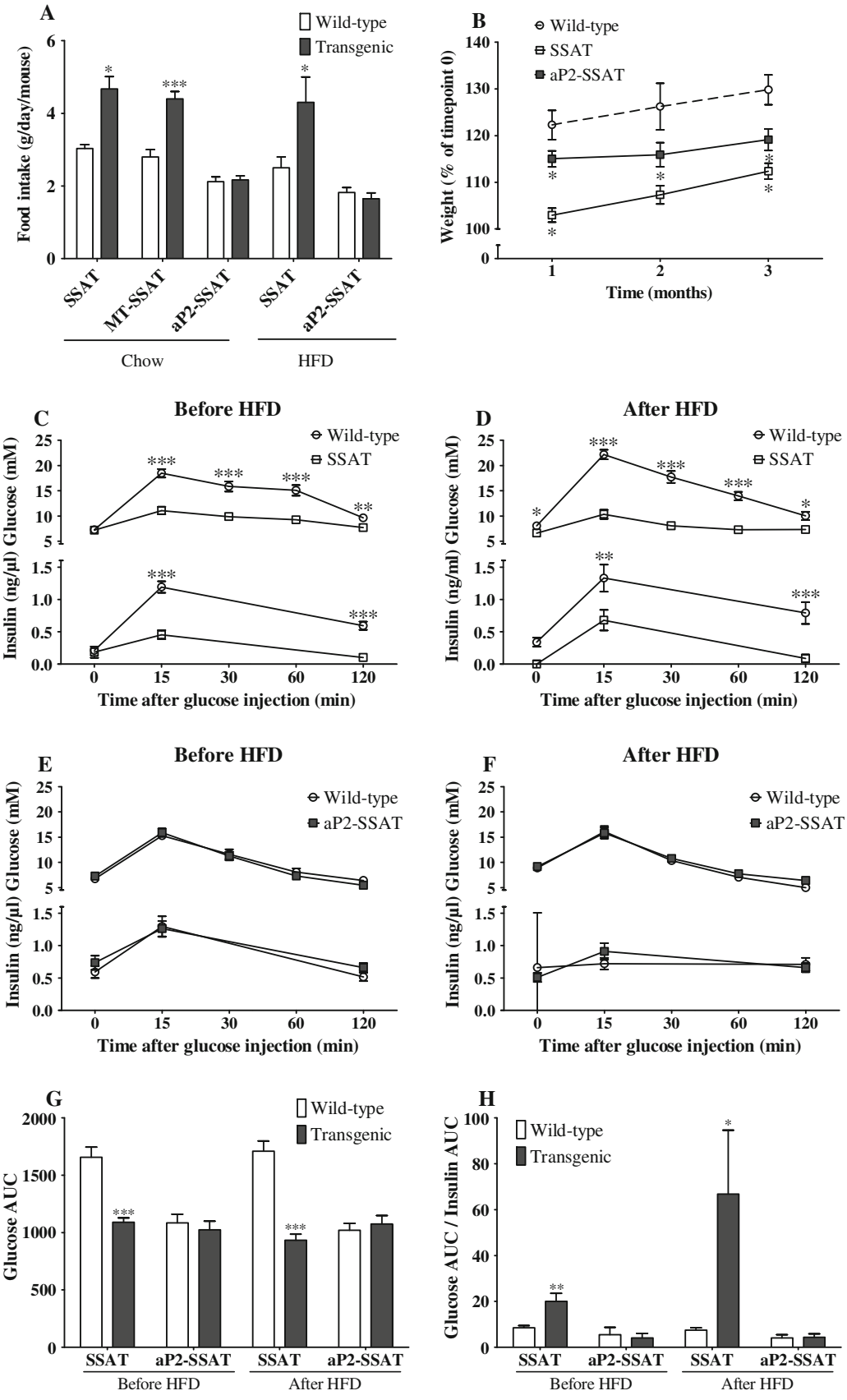
A
Wild-type
Transgenic
Food intake (g/day/mouse)
SSAT
MT-SSAT
aP2-SSAT
SSAT
aP2-SSAT
Chow
HFD
B
Wild-type
SSAT
aP2-SSAT
Weight (% of timepoint 0)
Time (months)
C
Before HFD
Wild-type
SSAT
Insulin (ng/µl) Glucose (mM)
Time after glucose injection (min)
D
After HFD
Wild-type
SSAT
Insulin (ng/ml) Glucose (mM)
Time after glucose injection (min)
E
Before HFD
Wild-type
aP2-SSAT
Insulin (ng/µl) Glucose (mM)
Time after glucose injection (min)
F
After HFD
Wild-type
aP2-SSAT
Insulin (ng/µl) Glucose (mM)
Time after glucose injection (min)
G
Wild-type
Transgenic
Glucose AUC
SSAT
aP2-SSAT
SSAT
aP2-SSAT
Before HFD
After HFD
H
Wild-type
Transgenic
Glucose AUC / Insulin AUC
SSAT
aP2-SSAT
SSAT
aP2-SSAT
Before HFD
After HFD

◀ **Fig. 4** High-fat diet results. **a** Food consumption during a standard chow or a high-fat diet. **b** Weight gain during the HFD. Glucose and insulin concentrations during the glucose tolerance test in SSAT ($N = 12$) **c** before and **d** after the HFD, and in the aP2-SSAT ($N = 17$) **e** before and **f** after the HFD. **g** AUC from the glucose levels during the glucose tolerance tests. The glucose tolerance tests were performed by injecting 12 h fasted mice intraperitoneally with 2 mg of D-glucose/g of body weight. Data are expressed as mean ± SEM. $*p < 0.05$, $**p < 0.005$, $***p < 0.0001$

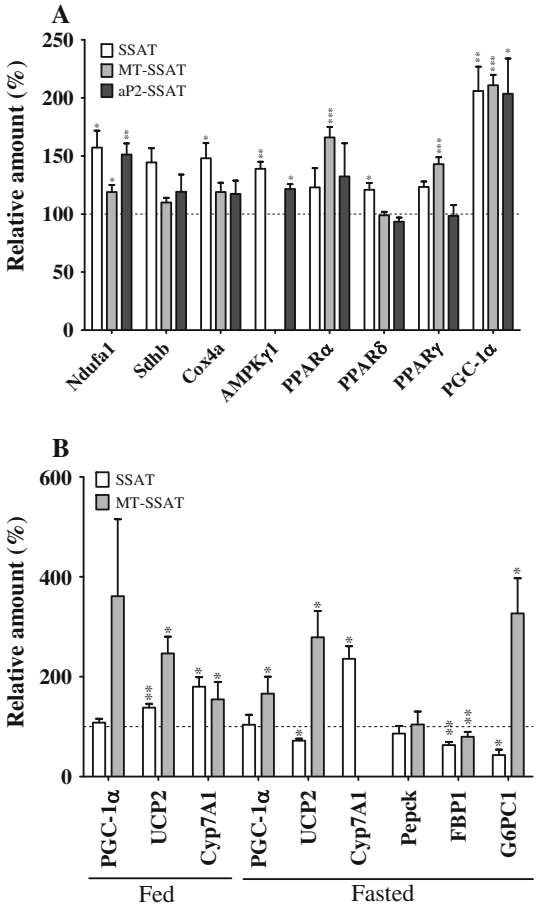

Fig. 5 mRNA expression profile of subcutaneous WAT and liver from three transgenic mouse lines with activated polyamine catabolism. Results are expressed as compared to wild-type values. **a** Subcutaneous WAT and **b** fed and fasted liver mRNA expression levels. Data are expressed as mean ± SEM from SSAT ($N = 8$) and MT-SSAT ($N = 5$). Data were normalized to the levels of β-actin. $*p < 0.05$, $**p < 0.005$, $***p < 0.0001$. Ndufa1, NADH-ubiquinone oxidoreductase MWFE subunit; Sdhb, succinate dehydrogenase Ip subunit; Cox4a, cytochrome c oxidase polypeptide IV; AMPKβ, 5′AMP-activated protein kinase subunit β; AMPKγ, 5′AMP-activated protein kinase subunit γ; PPARα, peroxisome proliferator-activated receptor α; PPARδ, peroxisome proliferator-activated receptor δ; PPARγ, peroxisome proliferator-activated receptor γ; PGC-1α, peroxisome proliferator-activated receptor gamma coactivator 1 alpha; UCP1, uncoupling protein 1; UCP3, uncoupling protein 3; UCP2, uncoupling protein 2; Cyp7A1, cholesterol 7 alpha hydroxylase; Pepck, phosphoenolpyruvate carboxykinase; FBP1, fructose-1,6-bis-phosphatase 1; G6PC1, glucose-6-phosphatase. SSAT data are reprinted with kind permission from the original publishers (Pirinen et al. 2007, 2010)

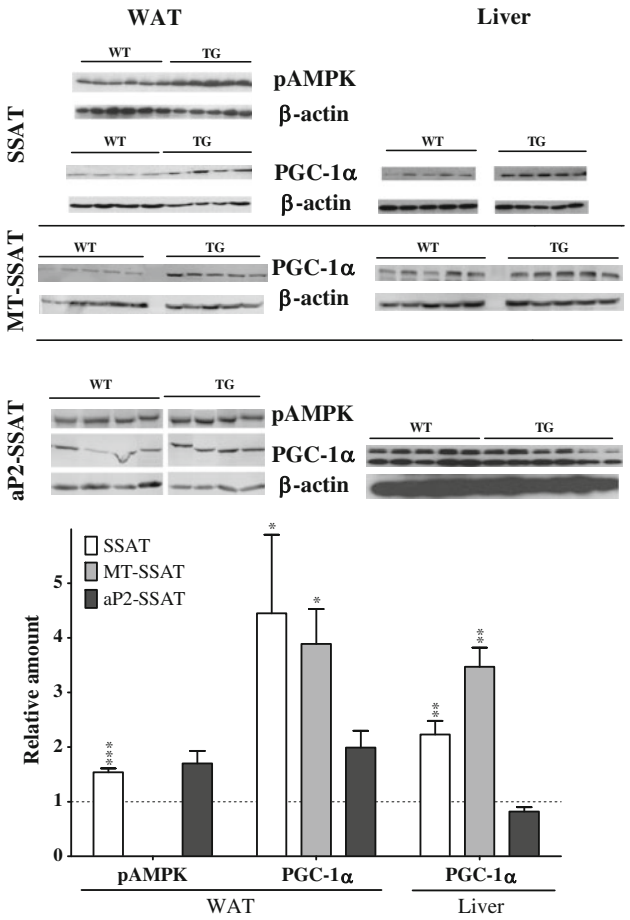

Fig. 6 Phosphorylated AMPK and PGC-1α protein expression levels in the WAT and liver from three transgenic mouse lines with activated polyamine catabolism. Actin levels were used for normalization and the results are compared to those of wild-type mice. SSAT ($N = 4$–6); MT-SSAT ($N = 5$); aP2-SSAT ($N = 5$–6). The MT-SSAT results are from male mice. The two different bands seen on the hepatic PGC-1α blot from the aP2-SSAT transgenic and wild-type mice correspond to different splice variants of the studied protein. $*p < 0.05$, $**p < 0.005$, $***p < 0.0001$. SSAT mice data are reprinted with kind permission from the original publishers (Pirinen et al. 2007, 2010)

Cyp7A1, which subsequently could lead to increased elimination of cholesterol from the organism. The activation of Cyp7A1 could be attributable to an increase in the activity and stability of the critical activator of bile acid synthesis, PGC-1α. Consistent with this hypothesis, PGC-1α protein and Cyp7A1 mRNA levels were increased in the livers of SSAT and MT-SSAT mice, but unaltered in aP2-SSAT mice (Pirinen et al. 2010). These findings demonstrate that lowered cholesterol levels are caused by the activation of hepatic polyamine catabolism, and that adipose tissue-specific polyamine catabolism activation does not influence the regulation of hepatic bile and cholesterol metabolism. When the SSAT and the aP2-SSAT mice were challenged with HFD, both transgenic lines were protected

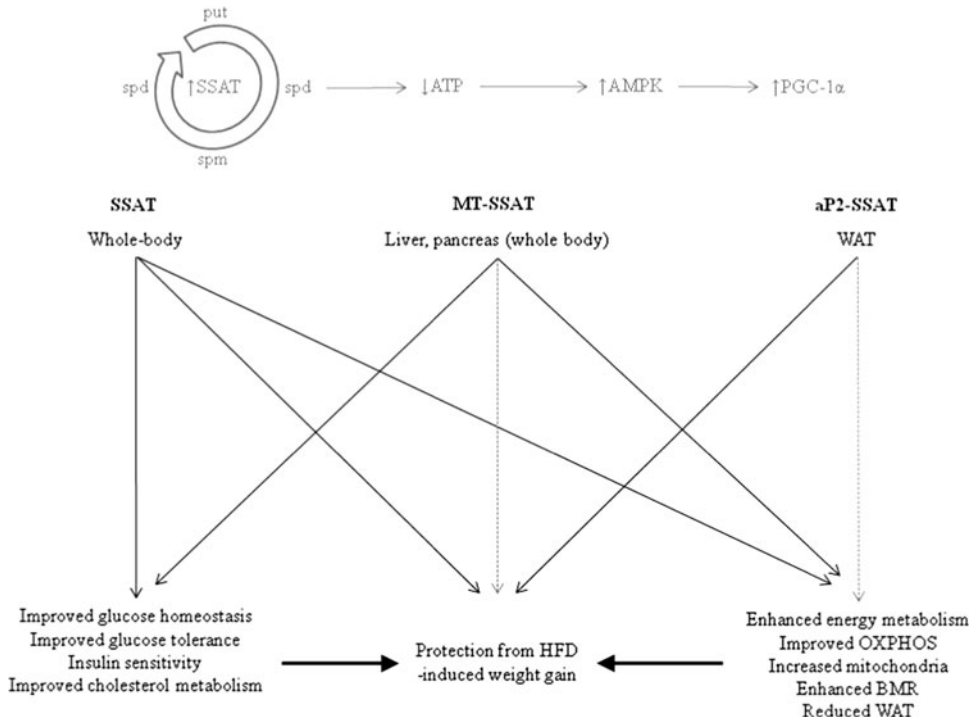

Fig. 7 Summary figure. Activation of polyamine catabolism produces a futile cycle that depletes the ATP pool. To reduce the energy consuming processes, AMPK becomes activated in the transgenic mice, ultimately leading to the activation of PGC-1α. Upon whole-body activation of the polyamine catabolism (SSAT and MT-SSAT mouse lines), glucose, energy and cholesterol metabolisms are stimulated, and glucose tolerance, insulin sensitivity, OXPHOS, BMR and number of mitochondria are enhanced. Furthermore, whole-body SSAT activation leads to significantly reduced WAT mass and circulating cholesterol levels, and protects against HFD-induced weight gain. However, when the activation of the polyamine catabolism is targeted to the WAT (aP2-SSAT mouse line), only some of the beneficial effects seen upon whole-body activation appear, such as protection against HFD, increased number of mitochondria and reduced WAT mass

from HFD-induced obesity, especially clearly for the SSAT mice. Surprisingly, SSAT mice treated with the HFD exhibited even further improved glucose tolerance than with the standard diet, whereas no improvement was detected in the aP2-SSAT mice. These results are in agreement with other mouse models overexpressing PGC-1α in the WAT that have been shown to be protected from HFD-induced weight gain due to enhanced energy expenditure (Tsukiyama-Kohara et al. 2001; Cederberg et al. 2001). Therefore, the current results clearly show that activated polyamine catabolism modulates energy balance and glucose metabolism even during an HFD.

We further verified that the beneficial effects on glucose and energy metabolism are at least partially mediated by the induction of AMPK and PGC-1α, as observed in the WAT of the three mouse models used in the current study. PGC-1α is the major regulator of mitochondrial biogenesis and energy expenditure (Puigserver et al. 1998), and becomes activated under conditions of increased energy demands and enhanced mitochondrial function mediated by AMPK. The elucidation of the pathways that control the activity of PGC-1α is crucial, as this information can be used to improve the metabolic control and prevent or treat diseases associated with abnormal mitochondrial activity. Consistent with this notion, our results support the hypothesis that the ideal concept for treating type 2 diabetes is to enhance energy expenditure through the activation of PGC-1α, and this is further associated with weight loss and beneficial changes in glucose homeostasis.

Altogether, we confirmed that the whole-body activation of polyamine catabolism has beneficial effects on glucose and energy homeostasis in mice, as reported earlier by Pirinen et al. (2007, 2010). More importantly, our findings advance the knowledge about the tissue specificity needed to influence glucose, energy and cholesterol metabolism. Activation of hepatic and skeletal muscle polyamine catabolism improved glucose and cholesterol homeostasis, while adipose tissue targeted enhanced polyamine catabolism was sufficient to protect mice from HFD diet-induced obesity. These observations are summarized in Fig. 7. Although, the whole-body activation of polyamine catabolism has severe side effects such as reduced life span, infertility and hairlessness (Pietilä et al. 1997; Suppola et al. 1999), adipose tissue-targeted enhanced polyamine

catabolism does not present these effects. Thus, adipose tissue-targeted SSAT overexpression could provide new possibilities for drug development, especially against obesity. To overcome the possible effect of non-targeted tissues, mice with skeletal muscle- or liver-specific overexpression of SSAT would be feasible study models in future studies. If the role of polyamine catabolism as a potential drug target is confirmed, the development of tissue-specific SSAT activators would be of interest, as currently there are only few strategies available to induce PGC-1α activity and energy expenditure. The modulable pathway that controls PGC-1α and energy expenditure in metabolically active tissues could provide a novel concept to prevent and/or treat metabolic diseases.

Acknowledgments We are grateful to Anne Karppinen, Arja Korhonen, Tuula Reponen, Sisko Juutinen, Marita Heikkinen, Teija Oinonen, Johanna Närväinen and Eila Ruotsalainen for their great technical assistance. This work was supported by grants from the Academy of Finland, the Finnish Cultural Foundation North Savo Regional Fund and the University of Eastern Finland's Doctoral Program in Molecular Medicine.

References

Attie AD, Kendziorski CM (2003) PGC-1alpha at the crossroads of type 2 diabetes. Nat Genet 34:244–245

Auwerx J (2006) Improving metabolisms by increasing energy expenditure. Nat Med 12:44–45

Benjamini Y, Hochberg Y (1995) Controlling the false discovery rate: a practical and powerful approach to multiple testing. J Roy Statist Soc Ser B 57:289–300

Cantó C, Auwerx J (2009) PGC-1alpha, SIRT1 and AMPK, an energy sensing network that controls energy expenditure. Curr Opin Lipidol 20:98–105

Cederberg A, Grønning LM, Ahrén B, Taskén K, Carlsson P, Enerbäck S (2001) FOXC2 is a winged helix gene that counteracts obesity, hypertriglyceridemia, and diet-induced insulin resistance. Cell 106:563–573

Cerrada-Gimenez M, Häyrinen J, Juutinen S, Reponen T, Jänne J, Alhonen L (2010) Proteomic analysis of livers from a transgenic mouse line with activated polyamine catabolism. Amino Acids 38:613–622

Cerrada-Gimenez M, Pietilä M, Loimas S, Pirinen E, Hyvönen MT, Keinänen TA, Jänne J, Alhonen L (2011) Continuous oxidative stress due to activation of polyamine catabolism accelerated aging and protects against hepatotoxic insults. Transgenic Res 20:387–396

Chomczynski P, Sacchi N (1987) Single-step method of RNA isolation by acid guanidinium thiocyanate–phenol–chloroform extraction. Anal Biochem 162:156–159

Du P, Kibbe WA, Lin SM (2008) Lumi: a pipeline for processing Illumina microarray. Bioinformatics 24:1547–1548

Gentleman RC, Carey VJ, Bates DM, Bolstad B, Dettling M, Dudoit S, Ellis B, Gautier L, Ge Y, Gentry J, Hornik K, Hothorn T, Huber W, Iacus S, Irizarry R, Leisch F, Li C, Maechler M, Rossini AJ, Sawitzki G, Smith C, Smyth G, Tierney L, Yang JY, Zhang J (2004) Bioconductor: open software development for computational biology and bioinformatics. Genome Biol 5:R80

Giles KW, Myers A (1964) The role of nucleic acids in the growth of the hypocotyl of *Lupinus albus* under varying light and dark regimes. Biochim Biophys Acta 87:460–477

Goldman SJ, Zhang Y, Jin S (2010) Autophagic degradation of mitochondria in white adipose tissue differentiation. Antioxid Redox Signal 14:1971–1978

Hammarstedt A, Jansson P, Wesslau C, Yang X, Smith U (2003) Reduced expression of PGC-1 and insulin-signaling molecules in adipose tissue is associated with insulin resistance. Biochem Biophys Res Commun 301:578–582

Hogan B, Constantini F, Lacy E (1986) Manipulating the mouse embryo. Cold Spring Harbor Laboratory, Cold Spring Harbor, NY

Hyvönen T, Keinänen TA, Khomutov AR, Khomutov RM, Eloranta TO (1992) Monitoring of the uptake and metabolism of aminooxy analogues of polyamines in cultured cells by high-performance liquid chromatography. J Chromatogr 574:17–21

Jänne J, Alhonen L, Pietilä M, Keinänen TA, Uimari A, Hyvönen MT, Pirinen E, Järvinen A (2006) Genetic manipulation of polyamine catabolism in rodents. J Biochem 139:155–160

Jell J, Merali S, Hensen ML, Mazurchuk R, Spernyak JA, Diegelman P, Kisiel ND, Barrero C, Deeb KK, Alhonen L, Patel MS, Porter CW (2007) Genetically altered expression of spermidine/spermine N1-acetyltransferase affects fat metabolism in mice via acetyl-CoA. J Biol Chem 282:8404–8413

Libby PR, Ganis B, Bergeron RJ, Porter CW (1991) Characterization of human spermidine/spermine N1-acetyltransferase purified from cultured melanoma cells. Arch Biochem Biophys 284:238–244

Lin SM, Du P, Kibbe WA (2008) Model-based variance-stabilizing transformation for illumina microarray data. Nucleic Acids Res 36:e11

McGarry FD, Brown NF (1997) The mitochondrial carnitine palmitoyltransferase system. From concept to molecular analysis. Eur J Biochem 244:1–14

Mootha VK, Lindgren CM, Eriksson K, Subramanian A, Sihag S, Lehar J, Puigserver P, Carlsson E, Ridderstråle M, Laurila E, Houstis N, Daly MJ, Patterson N, Mesirov JP, Golub TR, Tamayo P, Spiegelman B, Lander ES, Hirschhorn JN, Altshuler D, Groop LC (2003) PGC-1alpha-responsive genes involved in oxidative phosphorylation are coordinately downregulated in human diabetes. Nat Genet 34:267–273

Morino K, Petersen KF, Dufour S, Befroy D, Frattini J, Shatzkes N, Neschen S, White MF, Bilz S, Sono S, Pypart M, Shulman GI (2005) Reduced mitochondrial density and increased IRS-1 serine phosphorylation in muscle of insulin-resistant offspring of type 2 diabetic parents. J Clin Invest 115:3587–3593

Passonneau JV, Lowry OH (1993) Enzymatic Analysis: A Practical Guide. Humana Press, Ottawa

Patti ME, Butte AJ, Crunkhorn S, Cusi K, Berria R, Kashyap S, Miyazaki Y, Kohane I, Costello M, Saccone R, Landaker EJ, Goldfine AB, Mun E, DeFronzo R, Finlayson J, Kahn CR, Mandarino LJ (2003) Coordinated reduction of genes of oxidative metabolism in humans with insulin resistance and diabetes: potential role of PGC1 and NRF1. Proc Natl Acad Sci USA 100:8466–8471

Petersen KF, Dufour S, Befroy D, García R, Shulman GI (2004) Impaired mitochondrial activity in the insulin-resistant offspring of patients with type 2 diabetes. N Engl J Med 12:664–671

Petersen KF, Dufour S, Shulman GI (2005) Decreased insulin-stimulated ATP synthesis and phosphate transport in muscle of insulin-resistant offspring of type 2 diabetic parents. PLOS Med 2:e233

Pietilä M, Alhonen L, Halmekytö M, Kanter P, Jänne J, Porter CW (1997) Activation of polyamine catabolism profoundly alters tissue polyamine pools and affects hair growth and female

fertility in transgenic mice overexpressing spermidine/spermine *N*1-acetyltransferase. J Biol Chem 272:18746–18751

Pirinen E, Kuulasmaa T, Pietilä M, Heikkinen S, Tusa M, Itkonen P, Boman S, Skommer J, Virkamäki A, Hohtola E, Kettunen M, Fatrai S, Kasanen E, Koota S, Niiranen K, Parkkinen J, Levonen AL, Ylä-Herttuala S, Alhonen L, Smith U, Jänne J, Laakso M (2007) Enhanced polyamine catabolism alters homeostatic control of white adipose tissue mass, energy expenditure, and glucose metabolism. Mol Cell Biol 27:4953–4967

Pirinen E, Gylling H, Itkonen P, Yaluri N, Heikkinen S, Pietilä M, Kuulasmaa T, Tusa M, Cerrada-Gimenez M, Pihlakamäki J, Alhonen L, Jänne J, Miettinen TA, Laakso M (2010) Activated polyamine catabolism leads to low cholesterol levels by enhancing bile acid synthesis. Amino Acids 38:549–560

Puigserver P, Wu Z, Park CW, Graves R, Wright M, Spiegelman BM (1998) A cold-inducible coactivator of nuclear receptors linked to adaptive thermogenesis. Cell 92:829–839

Semple RK, Crowley VC, Sewter CP, Laudes M, Christodoulides C, Considine RV, Vidal-Puig A, O'Rahilly S (2004) Expression of the thermogenic nuclear hormone receptor coactivator PGC-1alpha is reduced in the adipose tissue of morbidly obese subjects. Int J Obes Relat Metab Disord 28:176–179

Smyth GK (2004) Linear models and empirical Bayes methods for assessing differential expression in microarray experiments. Stat Appl Genet Mol B 3: Article 3. http://www.bepress.com/sagmb/vol3/iss1/art3

Song J, Oh JY, Sung YA, Pak YK, Park KS, Lee HK (2001) Peripheral blood mitochondrial DNA content is related to insulin sensitivity in offspring of type 2 diabetic patients. Diabetes Care 24:865–869

Suppola S, Pietilä M, Parkkinen JJ, Korhonen VP, Alhonen L, Halmekytö M, Porter CW, Jänne J (1999) Overexpression of spermidine/spermine *N*1-acetyltransferase under the control of mouse metallothionein I promoter in transgenic mice: evidence for a striking post-transcriptional regulation of transgene expression by a polyamine analogue. Biochem J 338:311–316

R Development Core Team (2009) R: A language and environment for statistical computing. R Foundation for Statistical Computing, Vienna, Austria. ISBN: 3-900051-07-0. http://www.R-project.org

Tsukiyama-Kohara K, Poulin F, Kohara M, DeMaria CT, Cheng A, Wu Z, Gingras AC, Katsume A, Elchebly M, Spiegelman BM, Harper ME, Tremblay ML, Sonenberg N (2001) Adipose tissue reduction in mice lacking the translational inhibitor 4E-BP1. Nat Med 7:1128–1132

Vial G, Dubouchaud H, Leverve XM (2010) Liver mitochondria and insulin resistance. Acta Biochim Pol 57:389–392

Winder WW, Hardie DG (1999) AMP-activated protein kinase, a metabolic master switch: possible roles in type 2 diabetes. Am J Physiol 277:E1–E10